CFD Simulation and Comparison with Measurement of Steady Flow in Intake Ports and Combustion Chambers

B.A.Befrui

adapco
60 Broadhollow Road
Melville, New York 11747
USA

ABSTRACT

The aim of this paper is validation of the capability of computational fluid dynamic (CFD) method, as an engineering design tool, for investigation and optimization of the aerodynamic characteristics of intake port-combustion chamber assemblies. The predictive accuracy of the calculation method is assessed through simulation of stationary flow in various port-cylinder assemblies and comparison with the measured discharge coefficient, post-valve swirl number, in addition to detailed LDA measurements of the velocity distribution in the valve curtain and the combustion chamber. The extensive assessment of the calculations shows a consistent capability to predict the discharge coefficient to within experimental uncertainty. The trends of variation of swirl number with port configuration and valve lift is systematically predicted; however, the quantitative agreement is scattered.

INTRODUCTION

The aerodynamics of intake ports exert paramount influence on the engine breathing efficiency and the combustion characteristics. Over the last decade, the strive for a more fundamental understanding of the flow characteristics of intake systems - in conjunction with the experimental and computational studies of in-cylinder flow processes - simultaneous with the advances in non-intrusive laser diagnostic methods, resulted in various LDA measurements of flow distribution in the intake port-cylinder assemblies [1-6]. These studies provided valuable insight into the three dimensional flow structure in the intake ports and the substantial influence of the port-valve-cylinder configuration on the in-cylinder flow structure, mostly under steady flow conditions.

The multidimensional computational fluid dynamics (CFD) is rapidly emerging from its research status in automotive industry, to become an industrial design tool. However, the assimilation of CFD into design process, as an engineering tool for design evaluation and optimization prior to manufacture, requires validation of its predictive accuracy and limits of its application. This paper presents results of a systematic assessment of the current state-of-the-art computational fluid dynamic method for calculation of the flow characteristics of intake port-combustion chamber assemblies, through extensive simulation of production gasoline and diesel engine intake systems under stationary flow conditions.

The ultimate objective in application of CFD for engine combustion system development is the simulation of all components of engine internal flow (induction system, intake and exhaust ports, combustion chamber) under transient operating conditions, where extensive flow field investigation with the aid of experimental laser diagnostic methods is limited by optical access, measurement time and cost. However, the focus of the present study is assessment of the CFD method under stationary flow conditions, through quantitative comparison of the intake flow engineering parameters for which extensive data are available. There are several important reasons that warrant the present extensive validation study:

(i) The diversity of design and configuration of induction systems of practical interest, with distinct and complex flow characteristics, as for various direct and helical ports.

(ii) The sensitive dependence of port flow characteristics to intricate design and geometric features, that need to be accurately rendered by the computational mesh and reproduced by the calculations.

(iii) The various flow complexities of intake ports, with regard to known predictive limitations of turbulence models, such as three dimensional strain rate variation, strong streamline curvature, favorable and adverse pressure gradients, separation and compressibility effects.

(iv) The standard industry procedure for design and evaluation of port aerodynamics through established global performance parameters and the availability of extensive steady port flow data.

This paper presents results of a program of validation of the current standard CFD methodology, both with respects to the mathematical models and numerical practices, for a wide spectrum of intake port-combustion chamber assemblies of current production design, tolerance and geometric complexity. It also intends to provide guidelines for requisite mesh resolution and distribution in order to accurately render the geometry and resolve the flow.

The paper first explains important issues concerning the computational method and the present calculations, such as the boundary conditions. The computations and comparison with data are presented in the following section, in two parts: a detailed comparison of the velocity field of a helical port with LDA experimental data, and the collective comparison of the predicted and measured engineering parameters discharge coefficient and swirl number for eleven ports of diverse design. Finally, the important findings are highlighted in the conclusions.

THE COMPUTATIONAL METHOD

The commercial CFD code STAR-CD is used for the calculations. STAR-CD is a three dimensional elliptic-hyperbolic flow simulation code for steady/unsteady laminar and high/low Reynolds number turbulent flow in complex geometries with stationary/moving boundaries or interfaces within the solution domain.

The solution methodology of STAR-CD adopts a conservative finite volume discretization scheme, collocated variable storage arrangement and body-fitted, non-orthogonal coordinates [7] with non-structured and indirect addressed computational grids, which may be composed of hexahedral, tetrahedral or triangular prism cells. Also, local embedded mesh refinement capability is provided.

The method solves for the primitive variables using the SIMPLE pressure correction technique [8] for steady flows.

The calculations of intake port-combustion chamber flow used a high-Reynolds number k-ε turbulence model, employing the universal law-of-the wall for the near-wall low-Reynolds number flow region [9]. In majority of the calculations, the high order linear-upwind discretization method was used, after obtaining the results with upwind difference scheme, in order to minimize the numerical errors.

MODELING OF PORT-CYLINDER FLOWS

Flow Configuration

The investigation of eleven port-cylinder assemblies of diverse configuration are summarized in the present study. These include conventional direct and helical designs for the petrol and diesel engines, in addition to various new concepts for twin-intake configurations; examples of each category are shown in Figures 1(a) and 1(b). The surface meshes in Figure (1) also demonstrate the extensive use of STAR-CD non-structured, non-hexahedra computational mesh capability for accurate representation of the geometry and control of the mesh spatial density. In the more recent calculations, the imbedded mesh refinement capability was employed to resolve the details of valve-seat arrangement.

The calculations in this study employed computational meshes of order 150,000 - 530,000 cells; the higher mesh densities correspond to more recent calculations, made possible by affordable more resourceful computers. In spite of STAR-CD's mesh capabilities - which render redundant computational cells obsolete - this degree of mesh refinement was found necessary for accurate rendering of the geometry and for resolving the complex flow. Although a systematic mesh refinement was not attempted in any study, overall, the increase in the mesh density produced more satisfactory results.

Boundary Conditions

In accordance with the experimental procedure, two types of boundary conditions were used in the port flow calculations: the prescribed mass flow rate and the prescribed pressure drop. The imposition of prescribed mass flow rate boundary condition is straightforward: it is prescribed at the inlet and the conservation of mass is imposed at the solution domain outlet. The imposition of the (static) pressure drop boundary condition required more care, for, in general, the measurement conditions were not well defined (whether air blowing or sucking from ambient arrangement, the entrance and exit pressure losses of experimental rig, uncertainty associated with the measurement locations, etc.) or their use in the calculations involved a small error (e.g., imposition of wall-mounted pressure measurements, as uniform inlet and outlet conditions).

Evaluation of Global Parameters C_D and Swirl Number

The evaluation of discharge coefficient from the calculations is straightforward. It is calculated as:

(i) for prescribed mass flow condition

$$C_D = \frac{\text{prescribed mass flow rate}}{\text{ideal mass flow rate for the predicted pressure drop}}$$

(ii) for prescribed pressure drop

$$C_D = \frac{\text{predicted mass flow rate}}{\text{ideal mass flow rate for the prescribed pressure drop}}$$

The evaluation of swirl number from the calculated velocity field requires special care, since it depends on whether the paddle-wheel or torque-meter experimental technique is used for the measurement. The evaluation of the swirl number pertinent to the torque-meter measurement is straightforward: the net swirl momentum at the measurement plane is calculated with respect to the cylinder axis, using the predicted velocity field. In the case of paddle-wheel measurement of swirl number, the likely redistribution of axial momentum by the paddle-wheel must be taken into consideration. In the calculations, two extreme cases can be considered: zero axial momentum redistribution (i.e., the axial velocity profile does not change through paddle-wheel interaction) or maximum conversion of axial to radial/tangential momentum (i.e., a uniform axial velocity distribution exiting paddle-wheel). In the calculations presented, this influence is examined for one case; otherwise, the zero momentum redistribution assumption was adopted.

CALCULATIONS AND COMPARISON WITH DATA

Detailed Velocity Field Predictions

The predicted three dimensional velocity field for the helical port-cylinder assembly in Figure 2 are compared with the detailed LDA measurements of the three velocity components at several planes within the valve curtain and in the cylinder. Table 1 presents the range of valve lifts in the computational validation study and the availability of LDA data for comparison. The LDA data has rather fine spatial resolution, given the experimental difficulties, thus permitting detection of small scale feature of the flow structure; for instance, flow separation in the valve curtain or local vortical structures in the combustion chamber.

Figure 3(a) and 3(b) present a sample of the predicted velocity field in the valve opening region, and the measurement locations, for the valve lift of 12 mm. The most noteworthy feature of the flow is the large variation of the three dimensional velocity filed within the valve gap and around its periphery. In this respect, a number of relevant observations is worthwhile

(i) The fine resolution of the computational mesh is essential for accurate prediction of the flow field

(ii) The accurate position of the LDA measurement volume and its size (compared to the valve opening distance) are of extreme importance, since an inaccuracy of order 1 mm in measurement location can cause substantial error.

(iii) Certain flow field features, such as the separation in the valve opening, are of significance with respect to the port aerodynamic characteristics and in-cylinder flow structure [10].

Owing to space limitations, two representative samples of the velocity field predictions and measurements in the valve curtain and in the cylinder, for the valve lift of 12 mm, are presented in Figures 4 and 5. Figures 4(a), 4(b) and 4(c) show the predicted and measured distributions of axial, radial and tangential velocity components, respectively, at different planes (3, 5, 8, 11 mm from the cylinder head) within the valve opening. The extent of agreement between predictions and data is typical of all cases investigated.

The distributions of the axial and tangential velocity components in the cylinders at the measurement plane 140 mm from the cylinder head, are shown in Figures 5(a) and 5(b), respectively. The results depict the magnitude of the relevant velocity component around the circumference of concentric circles of 15, 30, 40, 50, 55, and 58 mm radii.

The comparison of the variations of global parameters CD and swirl number with valve lift, obtained from direct measurement and evaluated from CFD results, are presented in Figures 6(a) and 6(b). These show the extent of agreement of the global parameters, corresponding to the accuracy of the detailed velocity field displayed in Figure 5.

Results for Global Parameters C_D and Swirl Number

The comparison of the computations and measurement data for eleven port-cylinder assemblies, for which both the C_D and swirl number data were available, are shown in Figures 7 and 8. The results are displayed in the form of computed against measured values: also shown is the least square fit of the data and the axes bisector line indicating perfect agreement.

The results in Figure 7 show good correlation of the measured and predicted C_D for various port-cylinder configurations, over a wide range of valve lift variations. Notably, for each individual intake port, the prediction error (represented as the departure from the 45 degree bisector line) for the valve-lift range shows a consistent over/under prediction of C_D. This is interpreted as an indication of a systematic discrepancy, likely due to inaccuracy in the boundary conditions (such as imposition of discrete pressure data as uniform boundary conditions or difference in the manner of evaluation of discharge coefficient.

The comparison of the predicted and measured port swirl number in Figure 8, shows a systematic prediction of trends of variation with port design, over extensive valve lift ranges. However, the quantitative agreement is markedly scattered. The discrepancy can be attributed to a number of factors: the correctness of assumptions regarding the axial momentum redistribution for paddle-wheel swirl measurements; the influence of the presence of measuring device on the flow field, absent in the simulations; the large sensitivity of port swirl number, compared with discharge coefficient, to accurate prediction of the flow distribution in the valve curtain; and the uncertainty in the measurements.

Figure 9 highlights two influential causes of the scatter in the comparison of the predicted and measured port swirl number, for the case "F", displayed in Figure 8. It is remarkable that measurements of the port global aerodynamics on two identical paddle-wheel test rigs give similar C_D but substantially different values of swirl number, in particular at small valve lifts. The maximum uncertainty due to the assumption about the interaction of paddle-wheel with the axial flow distribution, in evaluation of the swirl number from the computations, is highlighted in Figure 9(b). It is notable that both uncertainties are significant and must be taken into consideration in the comparison of the predictions and data. Unfortunately, with the exception of case "F", no multiple test data was available for assessment of the uncertainty in the measurements.

CONCLUSIONS

The extensive validation study of the intake port-combustion chamber flow, under steady flow condition, shows that CFD method predicts the flow distribution closely, capturing the main features of the flow field. This is reflected in the prediction accuracy of the port global engineering parameters, C_D and swirl number.

The investigations show that discharge coefficient can be predicted to within experimental and computational (i.e., the boundary conditions) uncertainties. The trends of variation of flow swirl number in the combustion chamber with port configuration and the valve lift are systematically predicted. However, the quantitative agreement is scattered, likely owing to sensitivity to the flow field, measurement uncertainty and the procedure for evaluation of swirl number in the computations.

This study demonstrates that CFD, employing current standard modeling practices, provides a flexible and reliable tool for in-depth analysis of the aerodynamic features of port-combustion chamber assemblies. The application of more advanced turbulence models, such as the low Reynolds number k-ε and the Reynolds stress turbulence model, needs assessment for improving the predictive accuracy.

ACKNOWLEDGMENT

The author acknowledges colleagues at **adapco** for making available their calculation and several automotive companies for their permission for publication of these results.

REFERENCES

1. Brandstatter, W., Johns, R.J.R. and Wigley, A.; SAE Technical Paper 850 499, 1985.
2. Khalighi, B., El Tahry, S.H. and Kuziak, W.R. Jr.; SAE Technical Paper 860 462, 1986.
3. Arcoumanis, C., Vafidis, C. and Whitelaw, J.H.; J. Fluid Engineering, Vol. 109, 368-375, 1987.
4. Tindal, M.J., Cheung, R.S. and Yianneskis, M.; SAE Technical Paper 880 383, 1988.
5. Cheung, R.S.W., Nadarajah, S., Tindal, M.J. and Yianneskis, M.; SAE Technical Paper 900 058, 1990.
6. Höfler, T., Ahmadi Befrui, B. and Wigley, G.; Proc. Ninth Symposium on Turbulent Shear Flows, Paper 30.4, Kyoto, 1993.
7. Peric, M.; "A Finite-Volume Method for the Prediction of Three-Dimensional Fluid Flow on Complex Ducts," PhD Thesis, University of London, 1985.
8. Patankar, S.V. and Spalding, D.B.; Int'l. J. Heat Mass Transfer, Vol. 15, 1787, 1972.
9. Launder, B.E. and Spalding, D.B.; Mathematical Models of Turbulence, Academic Press, London, 1972.
10. Vafidis, C.; "Aerodynamics of Reciprocating Engines," PhD Thesis, University of London, 1985.

LOCATION	MEASUREMENTS	VALVE LIFT (mm)						
		2	4	6	8	10	12	14
VALVE CURTAIN	Radial velocity component			•		•	•	
	Tangential velocity component			•		•	•	
	Axial velocity component			•		•	•	
PLANE ONE Z = 70 mm	Radial velocity component			•			•	
	Tangential velocity component			•			•	
	Axial velocity component			•			•	
PLANE TWO Z = 140 mm	Radial velocity component			•			•	
	Tangential velocity component			•			•	
	Axial velocity component			•			•	
PLANE THREE Z = 168 mm	Radial velocity component							
	Tangential velocity component	•	•	•	•	•	•	•
	Axial velocity component	•	•	•	•	•	•	•
PLANE FOUR Z = 210 mm	Radial velocity component							
	Tangential velocity component	•	•	•	•	•	•	•
	Axial velocity component	•	•	•	•	•	•	•

Table 1: The flow investigations and availability of LDA data for the helical port (• indicates measurement is available).

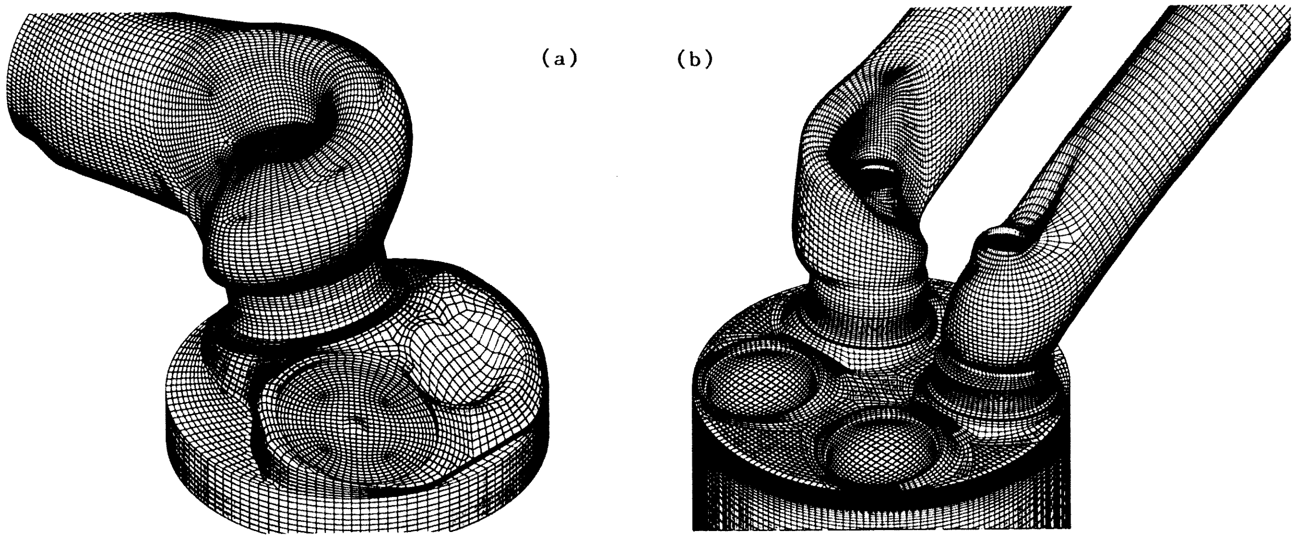

Figure 1: The geometry and computational mesh of intake port-cylinder assemblies for (a) single intake port, (b) twin intake port.

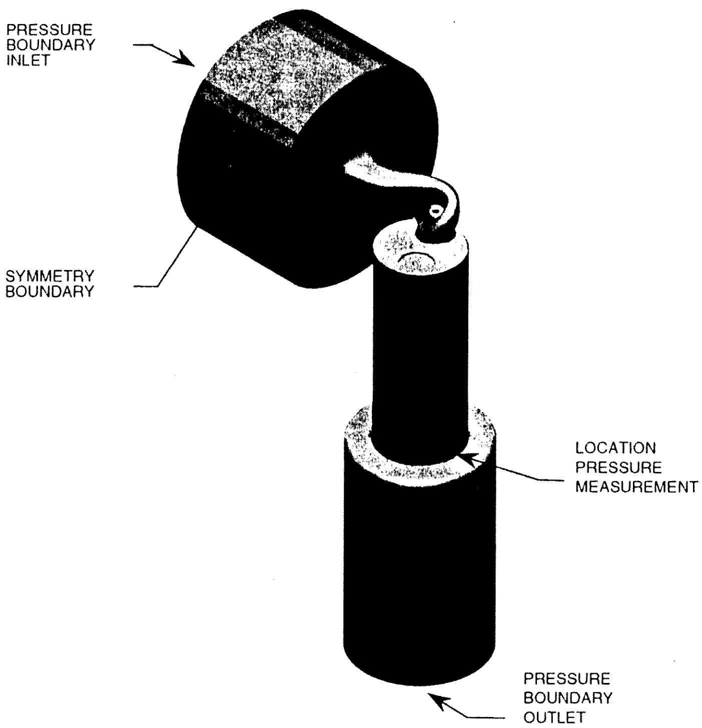

Figure 2: The configuration and experimental set up of the diesel helical port flow model.

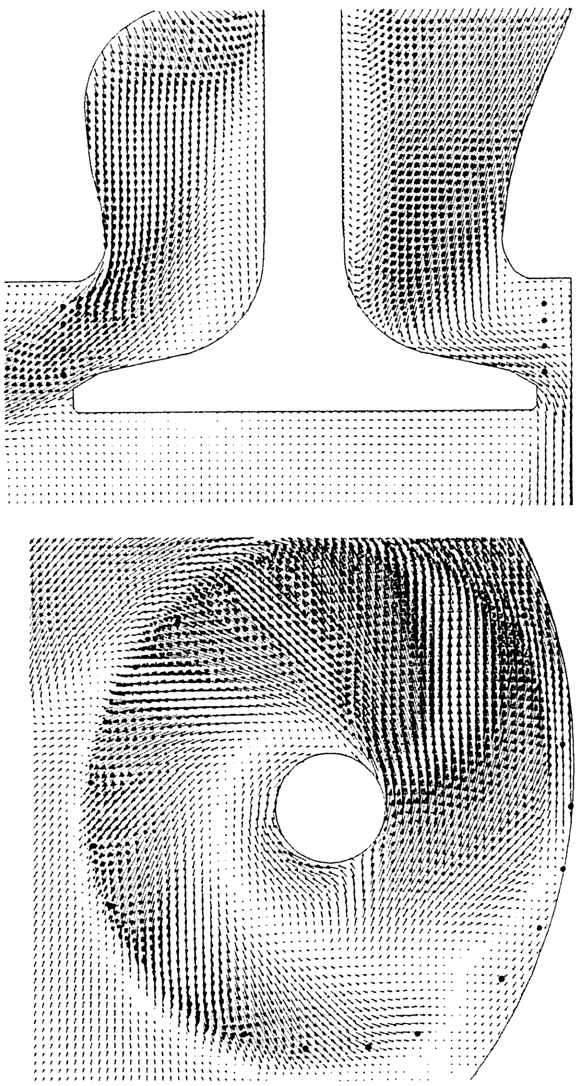

Figure 3: The predictions of the velocity field in the valve opening of the helical port (valve lift = 12mm).

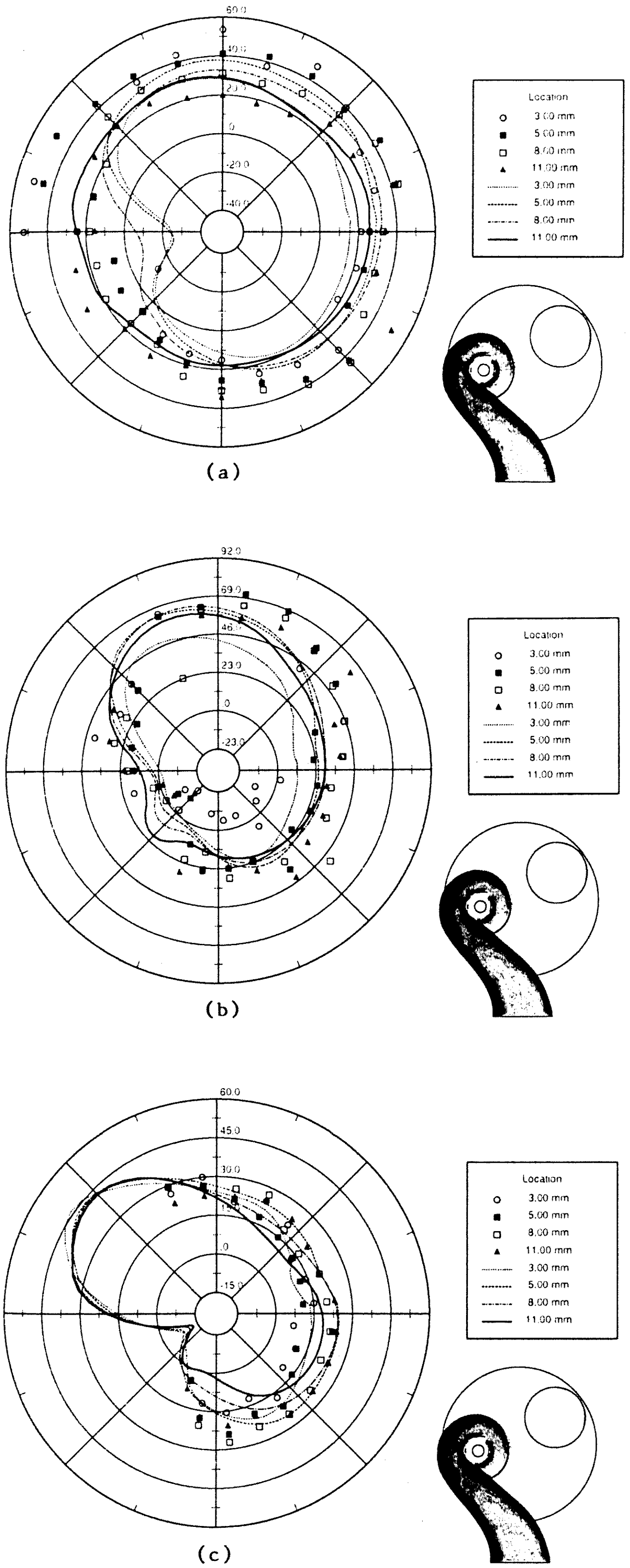

Figure 4: The comparison of the measured and predicted flow within the valve opening, for valve lift = 12 mm, for the helical port; (a) axial, (b) radial, (c) tangential velocity components.

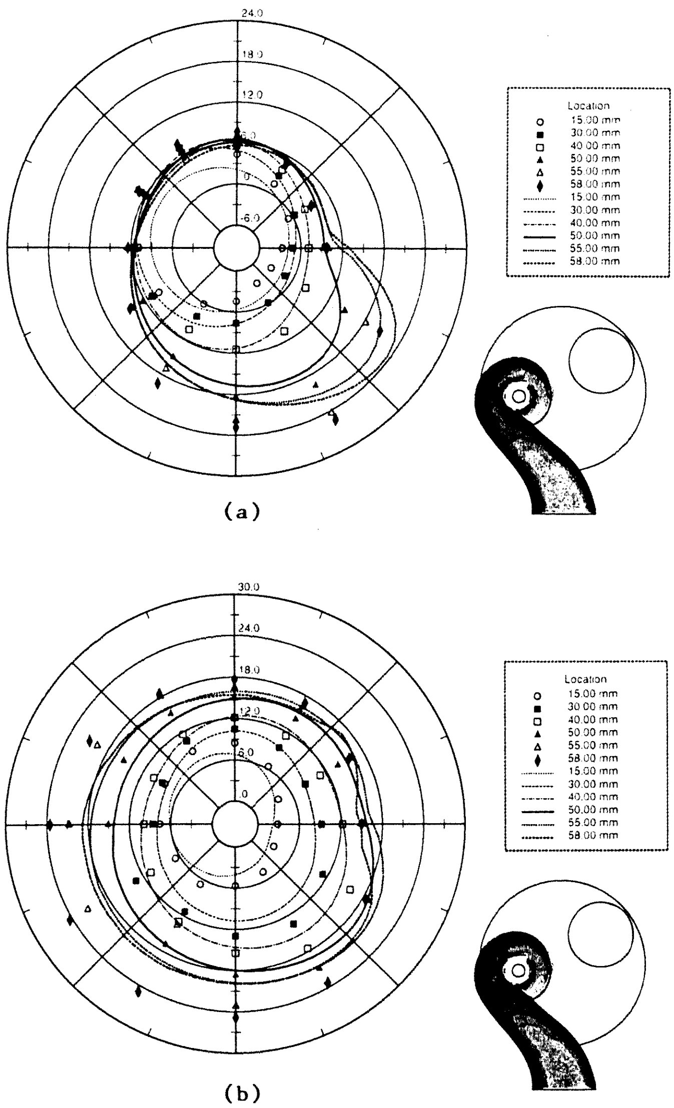

Figure 5: The comparison of the measured and predicted flow in the cylinder, at 140 mm from the cylinder head, for valve lift = 12 mm, for the helical port; (a) axial, (b) tangential velocity components.

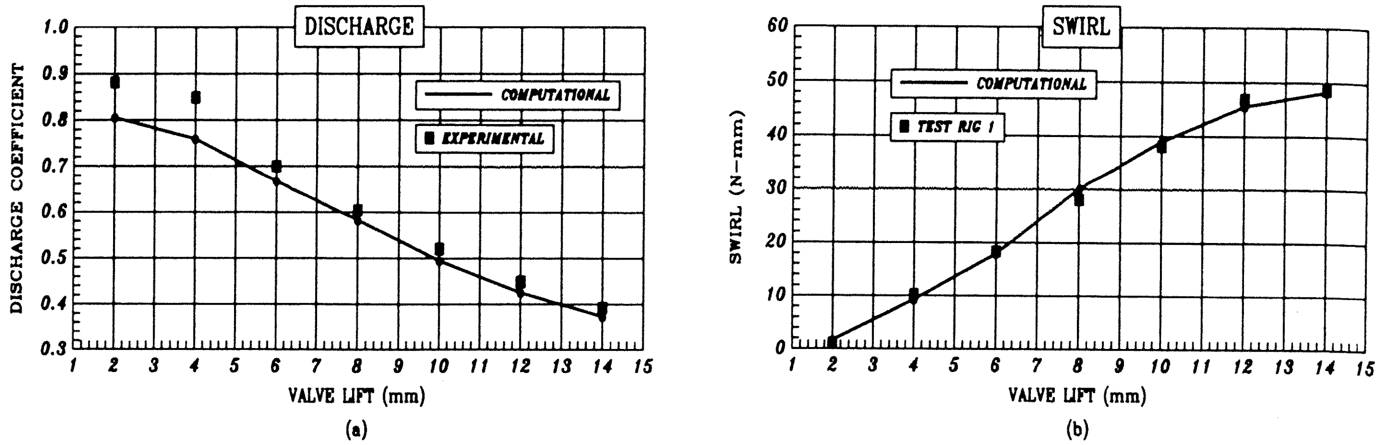

Figure 6: The comparison of measured and predicted variation of intake flow parameters with valve lift for the helical port, (a) discharge coefficient, (b) swirl number.

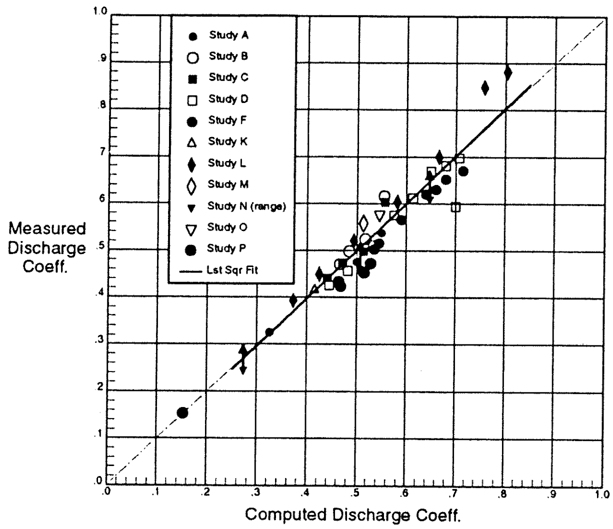

Figure 7: The collective comparison of the measured and predicted discharge coefficients for eleven ports.

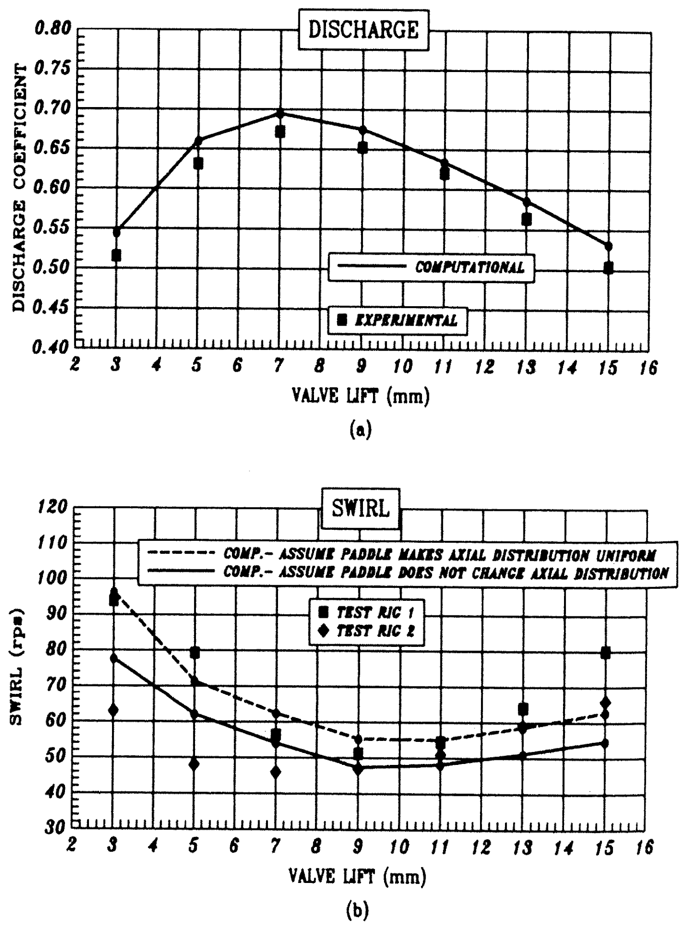

Figure 9: The uncertainties associated with the measurement data and method of calculation of global parameters for (a) discharge coefficient, (b) paddle-wheel swirl number.

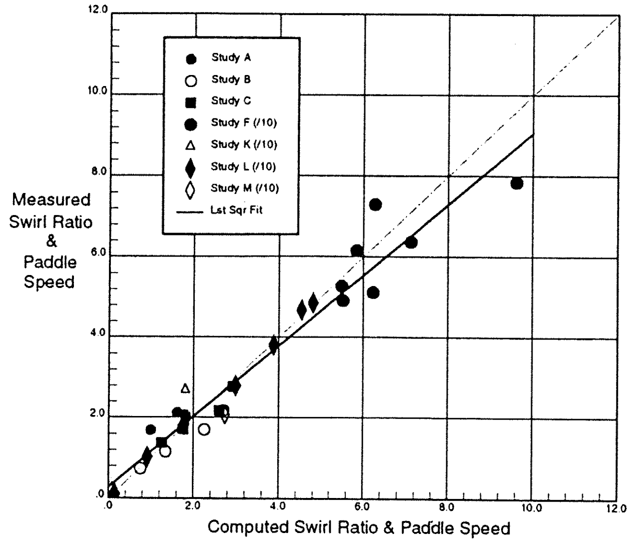

Figure 8: The collective comparison of the measured and predicted swirl number for seven ports.